Self-focusing of circularly polarized beams

Gadi Fibich and Boaz Ilan
Department of Applied Mathematics, Tel Aviv University, Tel Aviv, 69978, Israel
(Received 7 July 2002; revised manuscript received 14 October 2002; published 28 March 2003)

We present a systematic study of propagation of circularly polarized beams in a Kerr medium. In contrast to previous studies, vectorial effects (i.e., coupling to the axial component of the electric field and the grad-div term) and nonparaxiality are not neglected in the derivation. This leads to a system of equations that takes into account nonparaxiality, vectorial effects, and coupling to the opposite circular component (i.e., the one rotating in the opposite direction). Using this system we show that the standard model in the literature for self-focusing of circularly polarized beams can lead to completely wrong results, that circular polarization is stable during self-focusing, and that nonparaxiality and vectorial effects arrest collapse, leading instead to focusing-defocusing oscillations. We also show that circularly polarized beams are much less likely to undergo multiple filamentation than linearly polarized beams.

DOI: 10.1103/PhysRevE.67.036622 PACS number(s): 42.65.Sf, 42.65.Jx

I. INTRODUCTION

The nonlinear Schrödinger (NLS) equation is the model equation for self-focusing of *linearly polarized* beams in Kerr media. In 1965, Kelley used the NLS to predict the existence of a threshold power N_c, such that when the input power is above this threshold the beam would collapse (blow up) at a finite propagation distance [1]. The existence of a threshold power was confirmed experimentally (see Ref. [2], and references therein), providing support to the validity of the NLS model.

In 1966, Close, Giuliano, Hellwarth, Hess, McClung, and Wagner [3] conducted experiments with intense *circularly polarized* input beams propagating in Kerr media, which suggested that circular polarization is unstable. Close *et al.* also proposed a mathematical model for self-focusing of circularly polarized beams, which they used to explain the observed instability of circular polarization. Subsequent theoretical studies have used the same system of equations as Close *et al.*, but obtained contradictory results with regard to circular-polarization (in)stability. As a result, to date, there is some confusion in the literature with regard to circular-polarization stability. Remarkably, the only thing that was always agreed upon was the Close *et al.* model itself. As we show in this study, however, this model is based on problematic assumptions, and it can lead to wrong results.

The paper is organized as follows. In Sec. II, we review the vector Helmholtz model and the scalar NLS model for beam propagation in Kerr media. In Sec. III, we describe the contradictory results of previous studies on circular-polarization stability, all of which were based on the Close *et al.* system (9). In Sec. IV, we systematically reduce the vector Helmholtz equation to the system (19) that models self-focusing of circularly polarized beams. Similarly to the Close *et al.* system, system (19) takes into account the coupling to the opposite-circular component (i.e., the one rotating in the opposite direction). Unlike system (9), however, system (19) also takes into account beam nonparaxiality and *vectorial effects* (i.e., the contribution of the grad-div term and the coupling to the axial component). Using system (19), we show that circular-polarization is stable. We also show that the assumptions on which the derivation of the Close *et al.* system (9) is based can be physically incorrect. In Sec. V, we prove that when nonparaxiality and vectorial effects are negligible, the systems (9) and (19), as well as the simpler semidecoupled system (28), are asymptotically equivalent, and that solutions of these systems can undergo collapse. In Sec. VI, we use *modulation theory* to describe the dynamics of a single filament with the reduced system of ordinary differential equations (ODEs) (32), which shows that nonparaxiality and vectorial effects arrest beam collapse and lead to focusing-defocusing oscillations. In Sec. VII, we use numerical simulations of system (19) to confirm the stability of circular-polarization and the predictions of modulation theory. These simulations also demonstrate that the Close *et al.* system (9) can lead to wrong predictions.

Since the NLS equation is isotropic, according to the NLS model beams with cylindrically symmetric input profile should remain cylindrically symmetric during the propagation. However, experiments have shown that when the input power is much higher than N_c self-focusing dynamics can lead to multiple filamentation, i.e., beam breakup into several long and narrow filaments [4–6]. For over 35 years, the standard (and only) explanation for multiple filamentation, due to Bespalov and Talanov [7], has been that it is initiated by random noise in the input-beam profile. In Ref. [8], we showed that the symmetry breaking due to the preferred direction in the transverse plane which is induced by linear polarization can lead to a *deterministic* multiple filamentation, i.e., even when the input beams are perfectly cylindrically symmetric. In this study we show that, in contrast, cylindrically symmetric, *circularly polarized* input beams cannot undergo multiple filamentation, because in that case the input polarization state does not induce a preferred direction in the transverse plane. In Sec. VIII, we show that when the input profile is cylindrically symmetric, a small deviation from circular-polarization is unlikely to lead to multiple filamentation. However, small imperfections in the input profile, such as input noise or astigmatism, can lead to multiple filamentation. Finally, in Sec. IX, we compare self-focusing of circularly and linearly polarized beams. Based on our results, we predict that circularly polarized beams are much less

likely to undergo multiple filamentation than linearly polarized beams.

Note on notations. We use calligraphic letters ($\vec{\mathcal{E}}$, $\vec{\mathcal{P}}_{\rm NL}$, etc.) to denote dimensional variables and noncalligraphic letters ($\vec{E}$, $\vec{N}$, etc.) to denote dimensionless variables.

II. THE VECTORIAL MODEL

The propagation of intense cw laser beams in a Kerr medium is governed by the vector nonlinear Helmholtz equations

$$\Delta\vec{\mathcal{E}}(x,y,z)-\vec{\nabla}(\vec{\nabla}\cdot\vec{\mathcal{E}})+k_0^2\vec{\mathcal{E}}=-\frac{k_0^2}{\epsilon_0 n_0^2}\vec{\mathcal{P}}_{\rm NL}, \tag{1a}$$

$$\vec{\nabla}\cdot\vec{\mathcal{E}}=-\frac{1}{\epsilon_0 n_0^2}\vec{\nabla}\cdot\vec{\mathcal{P}}_{\rm NL}. \tag{1b}$$

Here $\vec{\mathcal{E}}=(\mathcal{E}_1,\mathcal{E}_2,\mathcal{E}_3)$ is the electric-field vector, $\vec{\mathcal{P}}_{\rm NL}$ is the nonlinear polarization vector, k_0 is wave number, ϵ_0 is vacuum permittivity, and n_0 is the linear index of refraction. When the Kerr medium is isotropic and homogeneous, the nonlinear polarization vector (i.e., the ''vector Kerr effect'') is given by [9,10]

$$\vec{\mathcal{P}}_{\rm NL}(\vec{\mathcal{E}})=\frac{4\epsilon_0 n_0\overline{n_2}}{1+\gamma}[(\vec{\mathcal{E}}\cdot\vec{\mathcal{E}}^*)\vec{\mathcal{E}}+\gamma(\vec{\mathcal{E}}\cdot\vec{\mathcal{E}})\vec{\mathcal{E}}^*], \tag{2}$$

where $\vec{\mathcal{E}}^*$ is the complex conjugate of $\vec{\mathcal{E}}$, $\overline{n_2}$ is the Kerr coefficient, and γ is a constant whose value depends on the physical origin of the Kerr effect.[1] Let us set the coordinate system such that the Kerr medium is located at the half space $z\geqslant 0$, the beam enters the Kerr medium at $z=0$ and propagates in the positive z direction.

Under the assumption that the beam is linearly polarized, i.e., $\vec{\mathcal{E}}=(\mathcal{E}_1(x,y,z),0,0)$, using the slowly varying envelope $\mathcal{E}_1=\mathcal{A}_1(x,y,z)e^{ik_0 z}$ and the paraxial approximation $\mathcal{A}_{1,zz}\ll k_0\mathcal{A}_{1,z}$, the vector Helmholtz model (1) reduces to the NLS equation,

$$2ik_0\mathcal{A}_{1,z}+\Delta_\perp\mathcal{A}_1+\frac{4k_0^2\overline{n_2}}{n_0}|\mathcal{A}_1|^2\mathcal{A}_1=0,$$

$$\mathcal{A}_1(x,y,z=0)=\mathcal{A}_1^0(x,y), \tag{3}$$

where $\Delta_\perp=\partial_{xx}+\partial_{yy}$. In dimensionless units, the NLS equation (3) is given by

$$i\psi_z(x,y,z)+\Delta_\perp\psi+|\psi|^2\psi=0,\quad \psi(x,y,z=0)=\psi^0(x,y). \tag{4}$$

Two important invariants of the NLS equation (4) are the power

$$N(z)=\int|\psi|^2dxdy=N(0),$$

and the Hamiltonian

$$H(z)=\int|\vec{\nabla}_\perp\psi|^2dxdy-\frac{1}{2}\int|\psi|^4dxdy=H(0), \tag{5}$$

where $\vec{\nabla}_\perp=(\partial_x,\partial_y)$. When the input power $N(0)$ is above a certain threshold N_c, solutions of Eq. (4) can collapse at a finite propagation distance.[2] The value of N_c is equal to the power of the so-called *Townes soliton* R, i.e., $N_c=2\pi\int_0^\infty R^2\,rdr\approx 2\pi\times 1.8623$ [13], where R is the positive solution of

$$R''(r)+\frac{1}{r}R'-R+R^3=0,\quad R'(0)=0,\quad \lim_{r\to\infty}R(r)=0, \tag{6}$$

and $r=\sqrt{x^2+y^2}$. For additional information on NLS collapse, we refer the reader to Refs. [14,15].

III. POLARIZATION (IN)STABILITY—HISTORICAL BACKGROUND

Strictly speaking, an intense circularly polarized input beam that propagates in a Kerr medium does not remain circularly polarized. Indeed, the vector Kerr effect (2) can be rewritten in terms of the circular components as

$$\vec{\mathcal{P}}_{\rm NL}(\vec{\mathcal{E}})=\frac{4\epsilon_0 n_0\overline{n_2}}{1+\gamma}[(|\mathcal{E}_+|^2+|\mathcal{E}_-|^2+|\mathcal{E}_3|^2)\vec{\mathcal{E}}$$

$$+\gamma(2\mathcal{E}_+\mathcal{E}_-+\mathcal{E}_3^2)\vec{\mathcal{E}}^*],$$

where the left-circular $(+)$ and right-circular $(-)$ components are denoted by

$$\mathcal{E}_\pm(x,y,z)=\frac{1}{\sqrt{2}}(\mathcal{E}_1+i\mathcal{E}_2), \tag{7}$$

and the corresponding input components are $\mathcal{E}_\pm^0(x,y)=\mathcal{E}_\pm(x,y,z=0)$. Thus, $\mathcal{E}_+$, $\mathcal{E}_-$, and $\mathcal{E}_3$ are nonlinearly coupled through the vector Kerr effect (2) and linearly coupled through the grad-div term in Eq. (1a). Therefore, even if initially $\mathcal{E}_-^0\equiv 0$, then $\mathcal{E}_-$ does not remain zero for $z>0$. In addition, in practice, the input beam is never perfectly circularly polarized. Therefore, a more realistic representation of circularly polarized input beams is $\mathcal{E}_+^0\gg\mathcal{E}_-^0$.

The above discussion motivates the following definition, which is later used in the analysis of the stability of circular-polarization.

[1]For example, $\gamma=0$ for electrostriction, $\gamma=1/2$ for nonresonant electrons, and $\gamma=3$ for molecular orientation.

[2]The condition $N(0)\geqslant N_c$ is necessary but not sufficient for collapse. The actual threshold power for collapse is generically a few percent above N_c for cylindrically symmetric input profiles [11], but can be considerably higher for anisotropic input profiles [12].

Definition (almost circularly polarized beam). A laser beam is said to be almost circularly polarized if $\mathcal{E}_- \ll \mathcal{E}_+$ and $\mathcal{E}_3 \ll \mathcal{E}_+$.

All previous studies of circular-polarization stability included the coupling of $\mathcal{E}_+$ to $\mathcal{E}_-$, but neglected the coupling of $\mathcal{E}_+$ to the axial component $\mathcal{E}_3$ and the grad-div term in Eq. (1a), i.e., they assumed that

$$\mathcal{E}_3 \ll \mathcal{E}_+, \quad \mathcal{E}_3 \ll \mathcal{E}_-, \quad \vec{\nabla}(\vec{\nabla}\cdot\vec{\mathcal{E}}) \ll k_0^2 \mathcal{E}_+. \tag{8}$$

Under the assumptions (8), Eqs. (1) and (2) reduce to the two coupled equations for $\mathcal{E}_+$ and for $\mathcal{E}_-$:

$$\Delta \mathcal{E}_\pm + k_0^2 \mathcal{E}_\pm + \frac{4k_0^2 n_2}{n_0(1+\gamma)}[|\mathcal{E}_\pm|^2 + (1+2\gamma)|\mathcal{E}_\mp|^2]\mathcal{E}_\pm = 0.$$

These studies also used the slowly varying envelopes $\mathcal{E}_\pm = \mathcal{A}_\pm(x,y,z)e^{ik_0 z}$ and the paraxial approximation $\mathcal{E}_{\pm,zz} \ll k_0 \mathcal{E}_{\pm,z}$, which lead to the two coupled equations for $\mathcal{A}_+$ and for $\mathcal{A}_-$:

$$2ik_0 \mathcal{A}_{\pm,z} + \Delta_\perp \mathcal{A}_\pm + \frac{4k_0^2 n_2}{n_0(1+\gamma)}[|\mathcal{A}_\pm|^2 + (1+2\gamma)|\mathcal{A}_\mp|^2]\mathcal{A}_\pm = 0. \tag{9}$$

System (9) has been used to determine whether circular-polarization is stable. As we now show, the results have been controversial.

A. The analysis of Close *et al.*

In 1966, Close *et al.* [3] conducted experiments with intense circularly polarized input beams propagating in Kerr media. They observed that "*in every case studied, the trapped light from a beam, circularly polarized to better than 1 part in 200, was markedly, if not completely, depolarized as soon as self-trapping could be detected.*" Moreover, "*the filament pattern [...] suggested that each filament might consist mainly of light linearly polarized in some random direction.*" In other words, they observed that circular-polarization is unstable and that during self-focusing circularly polarized beams formed filament(s) that are linearly polarized in randomly oriented directions. Close *et al.* suggested the following theoretical explanation for instability of circular polarization observed in their experiments. From system (9), it follows that the effective change of the nonlinear refractive index of $\mathcal{A}_\pm$ is given by

$$\delta n_\pm = \frac{4k_0^2 n_2}{n_0(1+\gamma)}[|\mathcal{A}_\pm|^2 + (1+2\gamma)|\mathcal{A}_\mp|^2]. \tag{10}$$

When $\gamma > 0$, the coefficient of the second term in the brackets of Eq. (10) is larger than the coefficient of the first term.[3] Therefore, Close *et al.* concluded that when $\gamma > 0$, self-focusing of the weaker-circular component is faster than that of the stronger-circular component. As a result, eventually a balance would be reached where $|\mathcal{A}_+| \approx |\mathcal{A}_-|$, which corresponds to linear polarization. Therefore, they concluded that linear polarization is stable, whereas circular-polarization is unstable.

B. Subsequent studies of system (9)

Wagner, Haus, and Marburger used the aberrationless approximation to approximate system (9) with a system of ODEs [17]. Based on these ODEs, they concluded that the self-focusing distance (i.e., the distance for beam collapse) is "sensitive" to small departures from circular polarization. This result suggests that circular-polarization is unstable. However, it was noted in Ref. [17] that the aberrationless approximation is a rough approximation of self-focusing dynamics.[4] Prakash and Chandra [18] as well as Vlasov, Korobkin, and Serov [19] studied system (9) and, using arguments similar to those in Ref. [3], reached the conclusion that both linear and circular polarizations are stable. These conclusions are consistent with the experimental observations of Meyer [20], as well as of Skinner and Kleiber [21], and of Golub, Shuker, and Erez [22].

In 1970, Berkhoer and Zakharov [23] showed that the power of each circular amplitude in system (9) is conserved during the propagation, i.e.,

$$N_\pm(z) = \int |\mathcal{A}_\pm|^2 dxdy = N_\pm(0). \tag{11}$$

This *proves* that according to system (9), circular polarization is stable[5] for both $\gamma > 0$ and $\gamma = 0$, because $N_+(z)/N_-(z) = N_+(0)/N_-(0) \gg 1$. In spite of this, the explanation of Close *et al.* for instability of circular-polarization has persisted in the nonlinear optics literature long after 1970 (e.g., in the classic book of Shen [16], Chap. 17), and even up to these days. Remarkably, the only thing that was always agreed upon is the system (9) itself. The derivation of system (9) is based, however, on the assumptions (8), which can be physically incorrect (see Sec. IV). Indeed, our simulations in Sec. VII show that system (9) can lead to completely wrong predictions.

IV. MODEL FOR SELF-FOCUSING OF CIRCULAR BEAMS

In this section, we present a systematic derivation of system (19) for propagation of circularly polarized input beams, which we derive from the vector Helmholtz model (1). Sys-

[3]Note that γ is positive for most liquids (Ref. [16], Chap. 17).

[4]It is now known that applying the aberrationless approximation to the two-dimensional (2D) NLS equation can lead to completely incorrect predictions [12]. Indeed, our numerical simulations in Sec. VII show that the self-focusing distance is relatively insensitive to the deviation from circular polarization (see footnote in Sec. VII).

[5]Strictly speaking, power conservation does not imply that the *intensity* of A_- does not become comparable to the intensity of A_+. However, the numerical simulations in Sec. VII show that A_- does remain much smaller than A_+ during the propagation, in contrast to the qualitative argument of Close *et al.*

tem (19) consists of two coupled equations for the two circular-polarization amplitudes, which, unlike the standard Close *et al.* model (9), also takes into account nonparaxiality, the contribution of the grad-div term, and the coupling to the axial component.

A key dimensionless parameter of the model is

$$f=\frac{1}{k_0 r_0}=\frac{\lambda}{2\pi r_0}, \tag{12}$$

where λ is wavelength and r_0 is input-beam width. Since the wavelength is much smaller than the input-beam width, the parameter f is small, i.e., $f\ll 1$. We are interested in the case where input beam is almost left-circularly polarized, i.e.,

$$\mathcal{E}_-^0/\mathcal{E}_+^0=O(\varepsilon),\quad \mathcal{E}_3^0\ll\mathcal{E}_+^0, \tag{13}$$

where ε measures the deviation from perfect input circular polarization. Therefore, there are two small parameters in the problem, i.e.,

$$f\ll 1 \quad \text{and} \quad \varepsilon\ll 1. \tag{14}$$

Since f and ε are small, we can use perturbation analysis to simplify the vector Helmholtz equation (1). To do this, we rescale the variables according to

$$\tilde{x}=\frac{x}{r_0},\quad \tilde{y}=\frac{y}{r_0},\quad \tilde{z}=\frac{z}{2L_{\mathrm{DF}}},$$

$$\vec{\mathcal{E}}=\frac{1}{2r_0k_0}\sqrt{\frac{n_0}{n_2}}\vec{A}(x,y,z)e^{ik_0z}, \tag{15}$$

where $\vec{A}=(A_1,A_2,A_3)$ is the dimensionless electric-field vector and $L_{\mathrm{DF}}=k_0r_0^2$ is the diffraction (''Rayleigh'') length. For convenience, we drop the tilde signs from now on. Using Eqs. (15), we rewrite the vector Helmholtz systems (1) and (2) in the dimensionless form (see Ref. [8])

$$i\vec{A}_{,z}+\Delta_\perp\vec{A}+\tfrac{1}{4}f^2\vec{A}_{,zz}+\vec{N}=-[f\vec{\nabla}_\perp+\hat{e}_3(i+\tfrac{1}{2}f^2\partial_z)][f\vec{\nabla}_\perp\cdot\vec{N}+iN_3+\tfrac{1}{2}f^2N_{3,z}], \tag{16a}$$

$$f\vec{\nabla}_\perp\cdot\vec{A}+iA_3+\tfrac{1}{2}f^2A_{3,z}=-f^2(f\nabla_\perp\cdot\vec{N}+iN_3+\tfrac{1}{2}f^2N_{3,z}), \tag{16b}$$

$$\vec{N}(\vec{A})=\frac{1}{1+\gamma}[(\vec{A}\cdot\vec{A}^*)\vec{A}+\gamma(\vec{A}\cdot\vec{A})\vec{A}^*], \tag{16c}$$

where $\hat{e}_3=(0,0,1)$ and $\vec{\nabla}_\perp=(\partial_x,\partial_y,0)$. In analogy with Eq. (7), we denote the nondimensional circular amplitudes by

$$A_\pm(x,y,z)=\frac{1}{\sqrt{2}}(A_1\pm iA_2) \tag{17}$$

and the corresponding input amplitudes by $A_\pm^0(x,y)=A_\pm(x,y,z=0)$.

Using a careful perturbation analysis of Eqs. (16), we prove in Sec. 1 of the Appendix the following result.

Lemma 1. Let an almost circularly polarized input beam [i.e., that satisfies Eq. (13)] propagate in a Kerr medium. Assume that the rescaling Eq. (15) is valid and that f and ε are small. Then the dimensionless amplitudes satisfy

$$A_-/A_+=O(f^2,\varepsilon) \tag{18a}$$

and

$$A_3/A_+=\frac{f}{\sqrt{2}}(iA_{+,x}+A_{+,y})+O(f^3,\varepsilon f). \tag{18b}$$

Since from Lemma 1 it follows that $A_-\ll A_+$ and $A_3\ll A_+$ for $z>0$, we have the following result.

Proposition 1 (stability of circular-polarization—part I). Under the assumption that the rescaling Eq. (15) is valid, an almost circularly polarized input beam remains almost circularly polarized during its propagation.

Proposition 1 shows that circular-polarization is stable, in agreement with Berkhoer and Zakharov [23] and in contrast to Close *et al.* [3]. Moreover, whereas the standard explanation of Close *et al.* for instability of circular-polarization assumes that $\gamma>0$, Proposition 1 is independent of the value of γ. An obvious weakness of Proposition 1 is that it is based on the assumption that the scaling (15) remains valid during the propagation. *A priori*, the validity of this assumption is questionable because of the high intensities that can be reached during self-focusing. However, in Sec. VI, we substantiate Proposition 1 by proving that Eq. (15) remains valid during self-focusing. Our numerical simulations in Sec. VII also corroborate this result.

We recall that all the previous studies used system (9), whose derivation is based on the assumption that $\mathcal{E}_3/\mathcal{E}_-\ll 1$. However, from estimates (18), it follows that $\mathcal{E}_-/\mathcal{E}_3=A_-/A_3=O(f,\varepsilon/f)$. Thus,

Corollary 1. When $\varepsilon\ll f$, the assumption that $\mathcal{E}_3\ll\mathcal{E}_-$ is wrong.

Indeed, in Secs. VI and VII, we show that system (9) leads to completely wrong predictions when $\varepsilon\ll f$. Moreover, we show that even when $f\ll\varepsilon$, this system can lead to wrong predictions.[6]

Using the estimates (18), we prove in Sec. 2 of the Appendix, the following result.

Proposition 2. Let an almost circularly polarized input beam [i.e., that satisfies Eq. (13)] propagate in a Kerr medium. Then to the leading order, $A_\pm(x,y,z)$ satisfy the coupled system,

[6]See, e.g., Fig. 3.

$$\underbrace{iA_{+,z}+\Delta_\perp A_+ +\frac{1}{1+\gamma}|A_+|^2A_+}_{\text{NLS for } A_+} = \underbrace{-\frac{1}{4}f^2A_{+,zz}}_{\text{nonparax.}} \underbrace{-\frac{1+2\gamma}{1+\gamma}|A_-|^2A_+}_{\text{coupling to } \mathcal{E}_-}$$

$$-\frac{f^2}{2(1+\gamma)}[\underbrace{4|\nabla_\perp A_+|^2A_+ +(\nabla_\perp A_+)^2A_+^* +|A_+|^2\Delta_\perp A_+ +A_+^2\Delta_\perp A_+^*}_{\text{vectorial effects}}], \quad (19a)$$

$$\underbrace{iA_{-,z}+\Delta_\perp A_-}_{\text{LS for } A_-} +\underbrace{\frac{1+2\gamma}{1+\gamma}|A_+|^2A_-}_{\text{coupling to } \mathcal{E}_+} =0, \quad (19b)$$

where

$$|\vec{\nabla}_\perp A_+|^2=|A_{+,x}|^2+|A_{+,y}|^2, \quad (\vec{\nabla}_\perp A_+)^2=A_{+,x}^2+A_{+,y}^2.$$

The terms that are neglected in Eqs. (19a) and (19b) are $O(f^4,\varepsilon f^2)$ and $O(f^2,\varepsilon^3)$, respectively.

Let us explain the origin of the terms in system (19). Equation (19b) is a linear Schrödinger (LS) equation for A_- with a nonlinear coupling to A_+ that results from the nonlinear coupling of $\mathcal{E}_+$ to $\mathcal{E}_-$ in Eqs. (1) and (2). When $\varepsilon=f=0$, system (19) reduces to the following NLS for A_+:

$$iA_{+,z}+\Delta_\perp A_+ +\frac{1}{1+\gamma}|A_+|^2A_+=0. \quad (20)$$

The $A_{+,zz}$ term on the right-hand side of Eq. (19a) is the nonparaxial term that comes from the scalar Helmholtz equation. The second term results from linear and nonlinear couplings of $\mathcal{E}_+$ to $\mathcal{E}_-$ in Eqs. (1) and (2). The remaining terms in Eq. (19a) result from vectorial effects, i.e., the contribution of the grad-div term and the coupling of $\mathcal{E}_+$ to $\mathcal{E}_3$. In Sec. VI, we show that the effect of the $O(f^2)$ terms, which are neglected in the Close *et al.* System (9), dominate the effect of the coupling to $\mathcal{E}_-$.

A. Contribution of the grad-div term

It is interesting to note that the $O(f^2)$ terms on the right-hand side of Eq. (19a) do not vanish even if one sets $\mathcal{E}_-\equiv\mathcal{E}_3\equiv 0$. Indeed, a close inspection of the derivation of this equation shows that in that case, the resulting equation for A_+, instead of Eq. (19a), is

$$iA_{+,z}+\Delta_\perp A_+ +\frac{1}{1+\gamma}|A_+|^2A_+ = -\frac{f^2}{4}A_{+,zz}-\underbrace{\frac{f^2}{2(1+\gamma)}\Delta_\perp(|A_+|^2A_+)}_{\nabla(\nabla\cdot(E_+,0,0))}. \quad (21)$$

The second term on the right-hand side of Eq. (21) corresponds to the contribution of the grad-div term in the vector Helmholtz equation (1a) when $\mathcal{E}_-\equiv\mathcal{E}_3\equiv 0$. This term can also be written as

$$\underbrace{-\frac{f^2}{2(1+\gamma)}\Delta_\perp(|A_+|^2A_+)}_{\nabla(\nabla\cdot(E_+,0,0))} \equiv -\frac{f^2}{2(1+\gamma)}[4|\nabla_\perp A_+|^2A_+ +2(\nabla_\perp A_+)^2A_+^* +2|A_+|^2\Delta_\perp A_+ +A_+^2\Delta_\perp A_+^*].$$

The remaining $O(f^2)$ terms in the square brackets on the right-hand side of Eq. (19a) correspond to the coupling to $\mathcal{E}_3$, both from the grad-div term and the nonlinear polarization field. To recapitulate, the $O(f^2)$ terms in the square brackets on the right hand side of Eq. (19a) correspond to the contribution of the grad-div-E_+ term and and the coupling to $\mathcal{E}_3$, i.e.,

$$\underbrace{\frac{f^2}{2(1+\gamma)}[4|\nabla_\perp A_+|^2A_+ +(\nabla_\perp A_+)^2A_+^* +|A_+|^2\Delta_\perp A_+ +A_+^2\Delta_\perp A_+^*]}_{\text{vectorial effects}} = \underbrace{\frac{f^2}{2(1+\gamma)}\Delta_\perp(|A_+|^2A_+)}_{\nabla(\nabla\cdot(E_+,0,0))} - \underbrace{\frac{f^2}{2(1+\gamma)}[(\nabla_\perp A_+)^2A_+^* +|A_+|^2\Delta_\perp A_+]}_{\text{coupling to } E_3}. \quad (22)$$

B. Power conservation

As mentioned in Sec. III B, Berkhoer and Zakharov [23] showed that the power of each circular amplitude is conserved in the system (9). The same holds, to leading order, in system (19), i.e.,

$$N_{\pm}(z)=\int |A_{\pm}|^2 dxdy = N_{\pm}(0)+O(f^2). \tag{23}$$

In other words, the power of each circular component is conserved with $O(f^2)$ accuracy. Since Eq. (13) implies that $N_-(0)/N_+(0)=O(\varepsilon^2)$, we conclude from Eq. (23) that $N_-(z)/N_+(z)=O(f^2,\varepsilon^2)$, i.e., that almost all of the beam's power remains in the left-circular component during the propagation. As we have noted, strictly speaking, power conservation does not imply that the *intensity* of A_- does not become comparable to the intensity of A_+. However, the numerical simulations of system (19) in Sec. VII show that A_- does remain $O(\varepsilon)$ smaller than A_+ during the propagation.

V. EARLY STAGE OF PROPAGATION

During the early stage of the propagation (i.e., at moderate levels of self-focusing), the $O(f^2)$ terms in system (19) are small, and the model can be simplified by setting $f=0$. The resulting system of equations is

$$iA_{+,z}+\Delta_{\perp}A_+ +\frac{1}{1+\gamma}[|A_+|^2+(1+2\gamma)|A_-|^2]A_+=0, \tag{24a}$$

$$iA_{-,z}+\Delta_{\perp}A_- +\frac{1+2\gamma}{1+\gamma}|A_+|^2A_-=0. \tag{24b}$$

Below we prove that solutions of Eq. (24) can undergo catastrophic collapse. Therefore, the simplified model (24) can be used for the early stage of the propagation, but fails to describe the propagation near and after the blow-up point.

We note the system (9) and (24) are almost identical,[7] the only difference being that the equation for A_- in system (9) includes the $|A_-|^2A_-$ term. This term is negligible, however, because it is $O(\varepsilon^2)$ smaller than the $|A_+|^2A_-$ term in Eq. (19b). Indeed, the numerical simulations in Sec. VII show that solutions of system (9) and (24) are almost indistinguishable.

A. Collapse of circularly polarized beams

We now prove that solutions of Eq. (24) can collapse at a finite propagation distance. To do that, we first observe that the system (24) conserves the two powers $N_+(z)$ and $N_-(z)$ as well as the Hamiltonian

$$H(z)=\int (|\vec{\nabla}A_+|^2+|\vec{\nabla}A_-|^2)dxdy - \frac{1}{2(1+\gamma)}\int |A_+|^4 dxdy - \frac{1+2\gamma}{2(1+\gamma)}\int |A_+|^2|A_-|^2 dxdy. \tag{25}$$

In addition, we have the following result.

Lemma 2 [variance identity for Eq. (24)]. Let $A_{\pm}(x,y,z)$ be the solution of Eq. (24) and let

$$V(z)=\int (|A_+|^2+|A_-|^2)(x^2+y^2)dxdy \tag{26}$$

be its variance. Then

$$V_{zz}=8H(z), \tag{27}$$

where $H(z)$ is defined by Eq. (25).

Equation (27) can be proved by differentiating $V(z)$ twice with respect to z, using Eq. (24) to replace z derivatives with transverse derivatives, and integrating by parts. As in the case of the NLS equation (4), from Hamiltonian conservation (25) and the variance identity (27) it follows that when $H(0)<0$, the variance would become negative at a finite propagation distance. Since by definition the variance has to be positive, this implies that the solution blows up at a finite propagation distance:

Proposition 3. Let $H(z)$ be given by Eq. (25). Then $H(0)<0$ is a sufficient condition for collapse of solutions of Eq. (24).

A similar result, of course, holds for system (9).

Proposition 4. Let $A_{\pm}(x,y,z)$ be the solution of system Eq. (9) and let $H(z)$ be given by

$$H(z)=\int (|\vec{\nabla}A_+|^2+|\vec{\nabla}A_-|^2)dxdy-\frac{1}{2(1+\gamma)}\int (|A_+|^4 + |A_-|^4)dxdy-\frac{1+2\gamma}{2(1+\gamma)}\int |A_+|^2|A_-|^2 dxdy.$$

Then $H(z)=H(0)$ and $V_{zz}=8H(z)$, where $V(z)$ is given by Eq. (26). Therefore, $H(0)<0$ is a sufficient condition for collapse of solutions of system Eq. (9).

Remark. Propositions 3 and 4 show that the coupling to $\mathcal{E}_-$ does not arrest the collapse. In fact, because the coupling term to A_- in the square brackets in Eq. (24a) appears with a positive coefficient, it *accelerates* the collapse.

B. Threshold power

Since the $|A_-|^2A_+$ term in Eq. (24a) is $O(\varepsilon^2)$ small as compared with the $|A_+|^2A_+$ term, to leading order, this term is negligible and system (24) can be further approximated with the semidecoupled system

$$iA_{+,z}+\Delta_{\perp}A_+ +\frac{1}{1+\gamma}|A_+|^2A_+=0, \tag{28a}$$

[7] Indeed, roughly speaking, $f=0$ corresponds to assumptions (8) and the paraxial approximation.

$$iA_{-,z}+\Delta_{\perp}A_{-}+\frac{1+2\gamma}{1+\gamma}|A_{+}|^{2}A_{-}=0. \tag{28b}$$

Here the equation for A_+ is decoupled from A_-. If we rescale A_+ in Eq. (28) as

$$\psi(x,y,z)=(1+\gamma)^{-1/2}A_{+}(x,y,z), \tag{29}$$

then Eq. (28a) becomes the NLS equation (4), showing that the threshold power for collapse of circularly polarized beams is

$$N_c^{\mathrm{circ}}=(1+\gamma)N_c. \tag{30}$$

VI. ASYMPTOTIC ANALYSIS

When the power of a laser beam is not much higher than N_c^{circ}, its propagation can be analyzed using *modulation theory* [24,14], which is an asymptotic theory for analyzing the effects of small perturbations on self-focusing in the 2D NLS equation (4).[8] Modulation theory is based on the observation that, after some propagation has taken place, a self-focusing beam rearranges itself as a modulated Townesian,[9] i.e.,

$$|A_{+}(x,y,z)|\sim\sqrt{1+\gamma}\,\frac{1}{L(z)}R\left(\frac{r}{L(z)}\right), \tag{31}$$

where $R(r)$ is defined in Eq. (6). Therefore, self-focusing dynamics is described by the modulation variable $L(z)$ that is proportional to beam width and to 1/(on-axis amplitude) as well. In particular, $L\to 0$ and $L\to\infty$ correspond to catastrophic collapse and to complete defocusing, respectively.

By applying modulation theory to system (19), we get that

Proposition 5. When $f,\varepsilon\ll 1$ and when the power of a circularly polarized laser beam is not much higher than N_c^{circ}, self-focusing dynamics is given, to leading order, by the reduced system of ODEs

$$L_{zz}(z)=-\frac{\beta}{L^{3}},$$

$$\beta_{z}(z)=-\frac{f^{2}(C_{\mathrm{nonparax.}}+C_{\mathrm{vec}})N_c}{2M}\left(\frac{1}{L^{2}}\right)_{z}+C_{E_{-}}(z), \tag{32}$$

where $|\beta|\ll 1$, $M=\frac{1}{4}\int_0^\infty\rho^2R^2\rho d\rho\approx 0.55$, $C_{\mathrm{nonparax.}}=1$, $C_{\mathrm{vec}}\approx 16/3$, *and* $C_{E_-}(z)=O(f^2,\varepsilon)$.

The proof of Proposition 5 is similar to that of Proposition 5.1 in Ref. [8]. For details, see Ref. [25].

[8]If the beam power is highly above N_c^{circ}, the beam can undergo multiple filamentation (see Sec. VIII). In that case, the power of each filament is slightly above N_c^{circ}, and the results of the asymptotic analysis can be applied to each filament.

[9]See, e.g., Fig. 2.

Inspection of the derivation of Eq. (32) shows that the terms with C_{nonparax}, C_{vec}, and $C_{E_-}(z)$ correspond to nonparaxiality, vectorial effects, and the coupling to $\mathcal{E}_-$ in Eq. (19a), respectively. Based on Eq. (32), we make the following observations.

(1) To leading order, nonparaxiality and vectorial effects have the same qualitative effect on self-focusing. This observation is surprising, because at the partial differential equation PDE level [i.e., system (19)] the expressions corresponding to nonparaxiality and vectorial effects are completely different.

(2) $C_{\mathrm{vec}}\approx 5.3C_{\mathrm{nonparax}}$. Thus, system (32) shows that vectorial effects are more than five times stronger than nonparaxiality.

(3) When $\varepsilon\ll 1$, the term corresponding to C_{E_-} is much smaller than the other terms in Eq. (32). Therefore, system (32) shows that the coupling to $\mathcal{E}_-$ is negligible as compared with nonparaxiality and vectorial effects. We thus see that *the Close et al. model* (9) *can be wrong even when* $\varepsilon\gg f$.

(4) Except for the small term that corresponds to the coupling to $\mathcal{E}_-$, system (32) is independent of γ. Indeed, if one neglects the coupling to $\mathcal{E}_-$ in Eq. (19a) and rescales A_+ as in Eq. (29), then γ is ''eliminated'' from the rescaled equation. Thus, we see again that *the value of* γ *(i.e., whether it is zero or positive) has no effect on circular-polarization stability*, in agreement with Berkhoer and Zakharov [23] and in contrast to Close *et al.* [3] (see Sec. III).

We now show that nonparaxiality and vectorial effects can arrest collapse. If we neglect the weak coupling to $\mathcal{E}_-$ (i.e., set $C_{E_-}=0$), we can follow [26,24] and integrate Eq. (32) to get that

$$(y_z)^2=-\frac{4H_0}{My}(y_M-y)(y-y_m),\quad y(z)=L^2(z), \tag{33}$$

where

$$y_m\approx\frac{M\beta(0)}{-2H_0}(1-\sqrt{1-4\delta})\sim\frac{f^2N_c(C_{\mathrm{nonparax.}}+C_{\mathrm{vec}})}{4M\beta(0)}[1+O(\delta)],$$

$$y_M\approx\frac{M\beta(0)}{-2H_0}(1+\sqrt{1-4\delta})\sim\frac{M\beta(0)}{-H_0}[1+O(\delta)], \tag{34}$$

$\delta=-f^2N_c(C_{\mathrm{nonparax.}}+C_{\mathrm{vec}})H_0/4M^2\beta^2(0)$, and $H_0\approx H(0)$, where $H(0)$ is the input Hamiltonian.

We recall that a necessary condition for collapse in the unperturbed NLS equation (28a), is that the input power is above threshold. In modulation theory variables [24], this condition amounts to $\beta(0)\approx[N(0)-N_c^{\mathrm{circ}}]/M\geq 0$. However, when $\beta(0)>0$ it follows from Eqs. (33) and (34) that $y(z)\geq y_m>0$. Therefore, collapse is arrested by nonparaxiality and vectorial effects, and the minimal beam width is $L_m\sim L(0)f\sqrt{N_c^{\mathrm{circ}}(C_{\mathrm{nonparax.}}+C_{\mathrm{vec}})/4M\beta(0)}$, which corresponds to several wavelengths. Since $\beta(0)\ll 1$, even at this

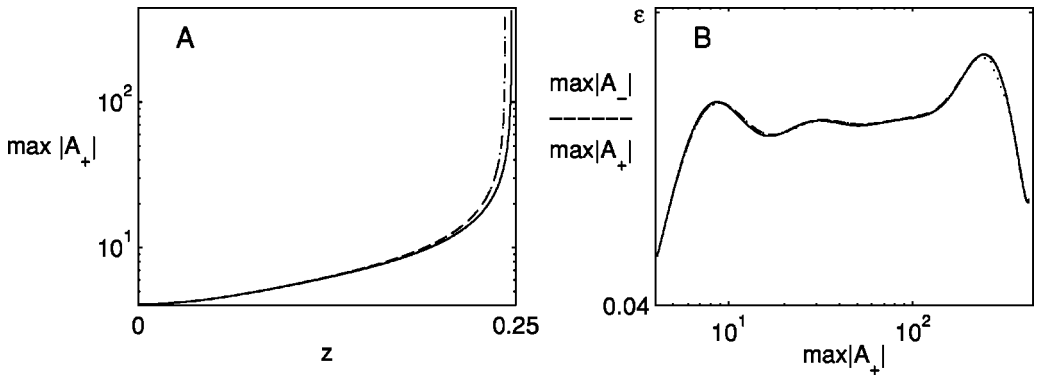

FIG. 1. Solutions of system (9) (dashed), system (24) (dotted), and system (28) (solid): (a) on-axis amplitude; (b) deviation from circular polarization. Here, $\gamma=0.5$ and the input beam is Eq. (35) with $\varepsilon=0.1$ and $N(0)=1.5N_c^{\mathrm{circ}}$.

stage the magnitude of the $O(f^2)$ terms in Eq. (19) is $O(\beta(0))$ smaller than that of the NLS terms $\Delta_\perp A_+$ and $|A_+|^2A_+$, providing an *a posteriori* justification for treating the right-hand-side terms in Eq. (19) as small perturbations:

Corollary 2. The scaling of the variables (15) remains valid during the propagation.

This enables us to remove the assumption in Proposition 1.

Proposition 6 (stability of circular-polarization—part II). When an almost circularly polarized beam [i.e., that satisfies Eq. (13)] with power moderately above N_c^{circ} propagate in a Kerr medium, the beam remains almost circularly polarized for all $z>0$.

In addition, a sufficient condition for collapse in the unperturbed NLS equation (4) is $H(0)<0$. However, from Eqs. (33) and (34), we see that if $\beta(0)>0$ and $H(0)<0$, then $y_m\leqslant y(z)\leqslant y_M$, i.e., arrest of collapse is followed by focusing-defocusing oscillations. When nonadiabatic radiation is added to Eq. (32), the oscillations decay during propagation [26]. A closer inspection of the derivation of Eq. (32) reveals that $C_{\mathrm{vec}}=C_{\vec{\nabla}(\vec{\nabla}\cdot(E_+,0,0))}+C_{E_3}$, where

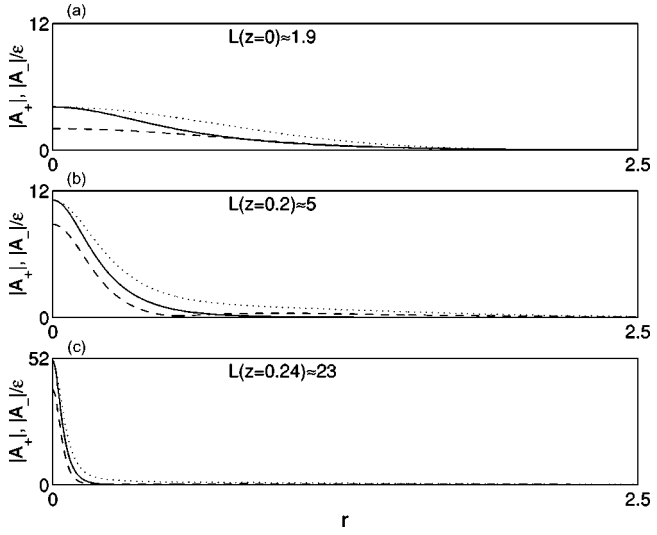

FIG. 2. $|A_+|$ (solid) converges to the modulated Townes profile (31) (dots) during beam collapse. The dashed line is $|A_-|/\varepsilon$. Data shown are the solution of system (24) in Fig. 1. (a) $z=0$, $L\approx0.5$; (b) $z=0.2$, $L\approx0.2$; (c) $z=0.24$, $L\approx0.04$.

$$C_{\vec{\nabla}(\vec{\nabla}\cdot(E_+,0,0))}\approx 8 \quad \text{and} \quad C_{E_3}\approx -\tfrac{8}{3}$$

correspond to contribution of $\mathcal{E}_+$ in the grad-div term (i.e., when $E_-=E_3=0$) and the coupling to $\mathcal{E}_3$, respectively. This result is surprising because it shows that the defocusing effect of $\mathcal{E}_+$ through the grad-div term is *eight times stronger* than nonparaxiality. Also surprising is that the coupling to $\mathcal{E}_3$ is *focusing*, since $C_{E_3}<0$. Indeed, since previous studies showed that vectorial effects arrest collapse (see, e.g., Refs. [27,8]), the general notion has been that the coupling to $\mathcal{E}_3$ is a defocusing mechanism. In contrast, our study shows that the coupling to $\mathcal{E}_3$ is, in fact, focusing, but the dominant vectorial effect, which is defocusing, results from the contribution of $\mathcal{E}_+$ to the grad-div term.

VII. STABILITY OF CIRCULAR-POLARIZATION SIMULATIONS

In this section, we confirm Proposition 6 and the predictions of modulation theory, by solving Eq. (19) for almost circularly polarized, Gaussian input beams

$$A_\pm^0(x,y)=\sqrt{N(0)}e^{-x^2-y^2}(1\pm e^{i\varepsilon}), \tag{35}$$

where the input power $N(0)=\int(|A_+|^2+|A_-|^2)dxdy$ is moderately above N_c^{circ}, see Eq. (30), and ε is the input "ellipticity angle" (i.e., $\varepsilon=0$ corresponds to a perfectly left-circularly polarized beam). Below we study different asymptotic regimes of the parameters f and ε.

Figure 1(a) confirms that when nonparaxiality and the coupling to the axial component are neglected (i.e., $f=0$), solutions of system (9), (28), and (24) can undergo catastrophic collapse, and that the solutions of these three systems are almost indistinguishable (see Sec. V). Figures 1(b) and 2 show that $A_-/A_+=O(\varepsilon)$, i.e., the solutions remain circularly polarized to leading order. Indeed, as the intensity of A_+ grows during the self-focusing process, the intensity of A_- also grows because of the coupling to A_+. However, A_- always remains smaller than A_+ (intuitively, because A_- has insufficient power for an independent collapse, see Sec. IV B). Figure 2 also confirms that A_+ approaches a modulated Townes profile during the collapse, thus justifying the application of modulation theory in Sec. VI.

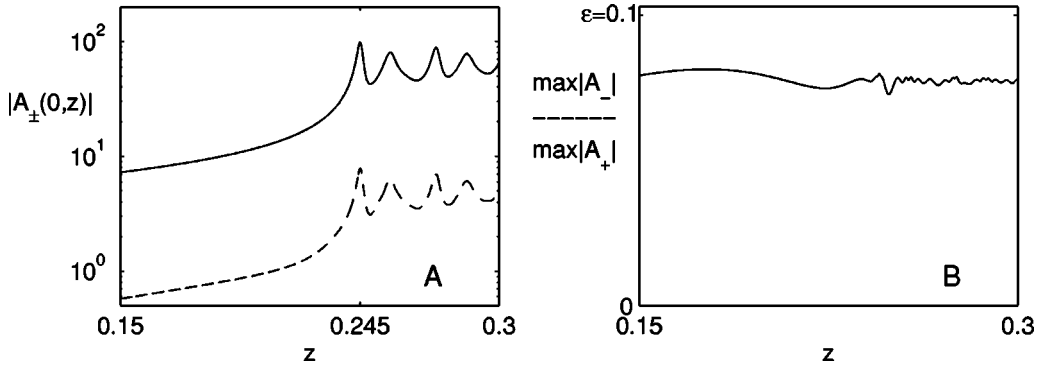

FIG. 3. Solutions of system (19): (a) on-axis amplitude of A_+ (solid) and of A_- (dashed); (b) deviation from circular-polarization. Same γ and input beam as in Fig. 1 with $f=0.01$ and $\varepsilon=0.1$.

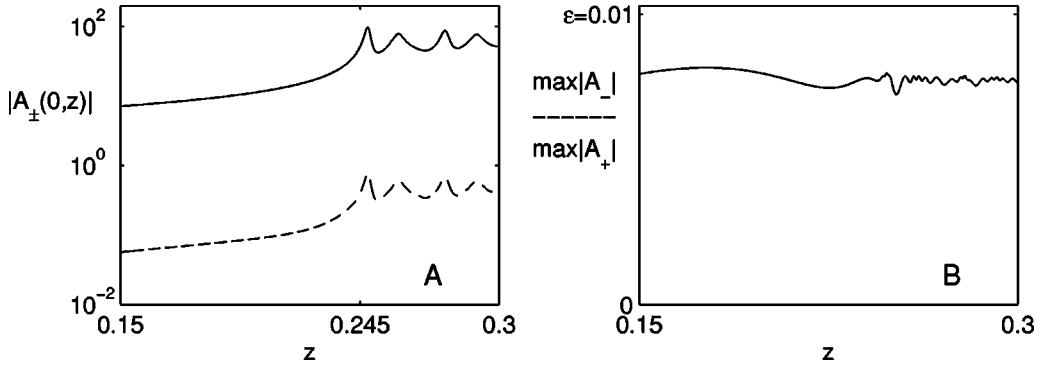

FIG. 4. Same as Fig. 3 with $f=\varepsilon=0.01$.

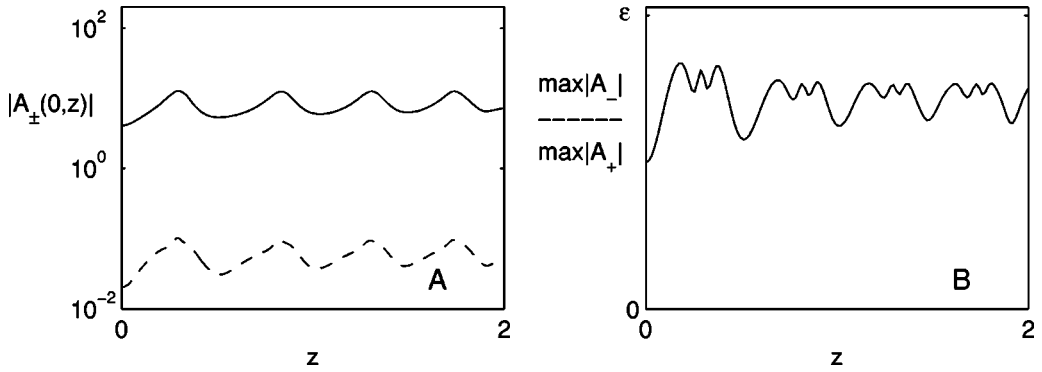

FIG. 5. Same as Fig. 3 with $f=0.1$ and $\varepsilon=0.01$.

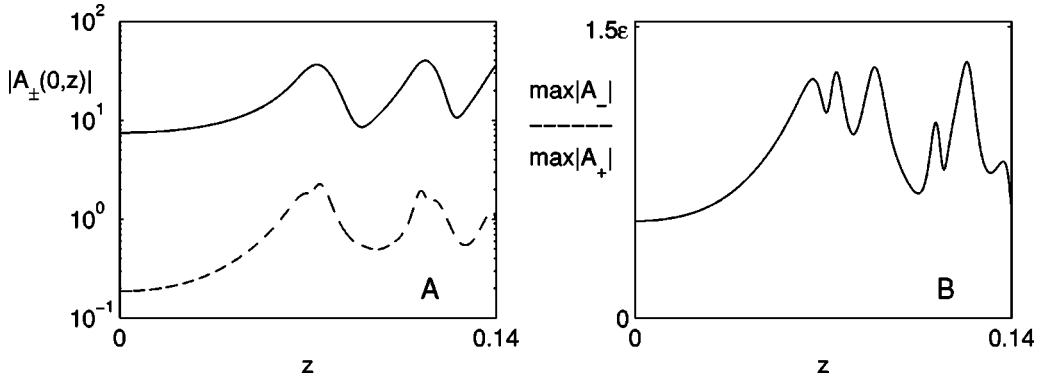

FIG. 6. Same as Fig. 3 with $N(0)=5N_c^{\mathrm{circ}}$ and $f=\varepsilon=0.05$.

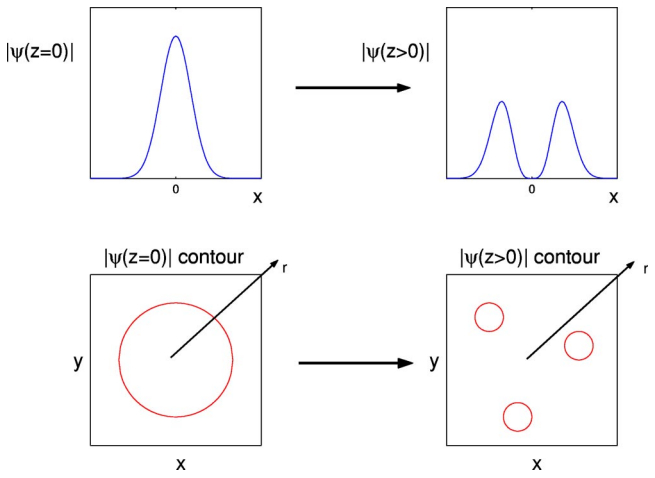

FIG. 7. Spatial symmetry can be maintained in 1D multiple filamentation (top) but not in 2D multiple filamentation (bottom).

When $0<f\ll\varepsilon$, one might expect that the coupling to A_- in Eq. (19) would dominate vectorial effects and nonparaxiality. In fact, quite the opposite is true. When $f>0$, the picture of self-focusing completely changes, because the $O(f^2)$ terms in Eq. (19), which correspond to nonparaxiality and vectorial effects, arrest beam collapse and lead to focusing-defocusing oscillations, as predicted by modulation theory in Sec. VI [see Fig. 3(a)]. In addition, the beam remains almost circularly polarized during propagation [see Fig. 3(b)]. Thus, even in this regime, system (9) leads to wrong predictions.

When $f=O(\varepsilon)$ and when $f\gg\varepsilon$, the picture is qualitatively similar to the case $0<f\ll\varepsilon$ (see Figs. 4 and 5). Moreover, the value of ε seems to have negligible quantitative effect on the dynamics of A_+, as can be seen by comparing Figures 3(a) and 4(a).[10] Finally, focusing-defocusing oscillations and circular-polarization stability are also observed when the input power is much higher than $N_c^{\rm circ}$ (see Fig. 6), a regime that is formally beyond the validity of modulation theory.

VIII. MULTIPLE FILAMENTATION

As noted in the Introduction, experiments with beams whose input power is highly above the self-focusing threshold can result in multiple filamentation, i.e., beam break up into several long and narrow filaments. We note that in 1D NLS models "multiple filamentation" can occur *without* breakup of the spatial symmetry.[11] In contrast, in 2D NLS models for beam propagation in a bulk Kerr medium, multiple filamentation *cannot* occur without breakup of cylindrical symmetry (see Fig. 7).

When an input profile is cylindrically symmetric, i.e., $A_\pm=A_\pm^0(r)$, then according to either the Close *et al.* model system (9) or our model (19), the beam remains cylindrically symmetric during the propagation, because these equations are isotropic. A natural question is therefore what is the symmetry-breaking mechanism that is responsible for multiple filamentation of circularly polarized input beams.

Let us first consider the "ideal" case of a circularly polarized input beam with a cylindrically symmetric profile. Since in this case neither the medium nor the input beam induce a preferred direction in the (x,y) plane, we can make the following observation.

Corollary 3. Let a circularly polarized, cylindrically symmetric input beam [i.e., $A_+^0=A_+^0(r)$ and $A_-^0=0$] propagate in a Kerr medium. Then the beam remains cylindrically symmetric during the propagation. In particular, the beam does not undergo multiple filamentation.

In the case of a cylindrically symmetric input profile [i.e., $A_\pm=A_\pm^0(r)$] with a small deviation from the circular-polarization state (i.e., $A_-^0\ll A_+^0$), the beam will not remain cylindrically symmetric during its propagation because the initial condition $(\mathcal{E}_+^0,\mathcal{E}_-^0)$ of the vector Helmholtz model (1) is not rotation invariant as a vector entity. In contrast, because Eqs. (19) are isotropic, when the input profile is cylindrically symmetric, then according to Eq. (19) the beam would remain cylindrically symmetric, i.e., $A_\pm=A_\pm(r,z)$ for all $z>0$. This "inconsistency" is due to the anisotropic $O(\varepsilon f^2)$ terms that are neglected in Eq. (19a), which account for the symmetry breaking in the Helmholtz model (1).[12]

Corollary 4. Let an almost circularly polarized, cylindrically symmetric input beam [i.e., $A_-^0\ll A_+^0$ and $A_\pm^0=A_\pm^0(r)$] propagate in a Kerr medium. Then to leading order, the beam remains cylindrically symmetric during the propagation, i.e., $A_+=A(r,z)+O(\varepsilon f^2)$ for all $z>0$.

Corollary 4 suggests that cylindrically symmetric, almost circularly polarized beams would not undergo multiple filamentation. This result is not conclusive, of course, as Eq. (19) neglects the $O(\varepsilon f^2)$ symmetry-breaking terms in the vector Helmholtz model (1). Indeed, in the "extreme" case of linear polarization (i.e., $\varepsilon=1$), these $O(f^2)$ symmetry-breaking terms can lead to multiple filamentation (see Sec. IX).

A. Scalar equation for circularly polarized beams

In Corollaries 3 and 4, we assumed that the input beam is cylindrically symmetric. Such idealization, however, is unrealistic, as there is always some degree of imperfection when generating an input beam. Since the coupling to A_- in Eq. (19a) is $O(\varepsilon^2)$ small (see Sec. V B), system (19) can be approximated with the scalar equation

[10]This comparison also shows that the deviation from circular-polarization has a small effect on the location of the (first) focal point (see footnote in Sec. III B).

[11]For instance, when two identical 1D solitons move toward each other and overlap at $z=0$, then at $z=0$ the input intensity is spatially symmetric, yet, according to the 1D NLS, there would be two distinct solitons at a sufficiently large propagation distance.

[12]A close inspection of the derivation of Eq. (19) shows that the $O(f^4)$ terms that are neglected in Eq. (19a) are isotropic, because they correspond to higher-order effects of nonparaxiality and the coupling of $\mathcal{E}_+$ to $\mathcal{E}_3$.

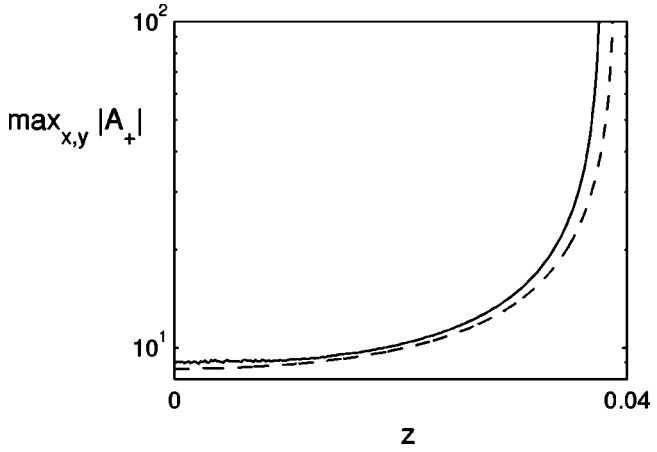

FIG. 8. Peak amplitude of the solution of system (9) with the noisy input beam (37) with $\varepsilon=0.1$, $c=0.1$ (i.e., 10% noise), and $N(0)=10N_c^{\mathrm{circ}}$ (solid). Also shown is the solution with the same input beam but without the noise (i.e., $c=0$, dashed).

$$iA_{+,z}+\Delta_\perp A_+ + \frac{1}{1+\gamma}|A_+|^2A_+ = -\frac{1}{4}f^2A_{+,zz} - \frac{f^2}{2(1+\gamma)}[4|\vec{\nabla}_\perp A_+|^2A_+ + (\vec{\nabla}_\perp A_+)^2A_+^* + |A_+|^2\Delta_\perp A_+ + A_+^2\Delta_\perp A_+^*]. \quad (36)$$

In Secs. VIII B and VIII C, we use Eq. (36) to study whether small imperfections in the input profile can lead to multiple filamentation of circularly polarized beams.

B. Noise-induced multiple filamentation

The standard theoretical explanation of multiple filamentation (of linearly polarized beams) was suggested by Bespalov and Talanov in 1966 [7]. According to that model, multiple filamentation is initiated by the noise in the input-beam profile that breaks up the cylindrical symmetry. In order to test whether noise can lead to multiple filamentation of circularly polarized beams, we first solve the Close *et al.* system (9) with very high-power input beams, to which we add noise both in amplitude and in phase, i.e.,

$$A_\pm^0(x,y)=\sqrt{N(0)}e^{-(x^2+y^2)}(1\pm e^{i\varepsilon})[1+cP(x,y)], \quad (37)$$

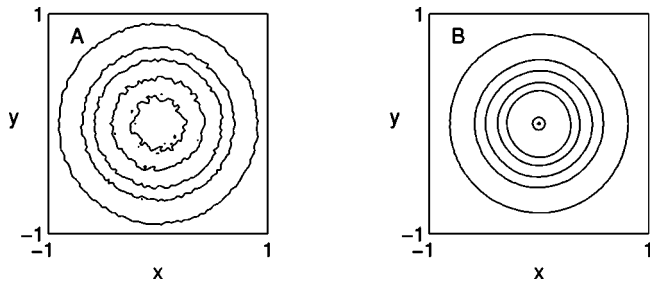

FIG. 9. Contour plots of the noisy solution of Fig. 8. (a) $|A_+(x,y,z=0)|$; (b) $|A_+(x,y,z=0.036)|$.

where $N(0)$ is the noiseless input power, $P(x,y)$ is a random complex-valued function, and the constant c determines the noise level. In our simulations, we see neither evidence for multiple filamentation nor even for mild instabilities. Rather, the beam collapses while converging to a cylindrically symmetric profile (see Figs. 8 and 9). We do see, however, multiple filamentation when we solve Eq. (36) with noisy high-power input beams, i.e.,

$$A_+^0(x,y)=2\sqrt{N(0)}e^{-(x^2+y^2)}[1+cP(x,y)], \quad (38)$$

where $N(0)$ is several times N_c^{circ}. For example, in Figs. 10–12, we show a noisy beam with ten times the threshold power that breaks up into three filaments.[13] Note that the difference between the scalar equation (36) and the Close *et al.* system (9) is the $O(f^2)$ nonparaxial and vectorial effects terms, both of which are isotropic. Thus, these terms cannot lead to multiple filamentation by themselves. Nevertheless, as the above simulations show, they are necessary for noise-induced multiple filamentation, (see Sec. IX B for further discussion).

C. Astigmatism induced multiple filamentation

Optical devices, such as those used for producing circularly polarized beams, are known to produce astigmatic beams (see, e.g., Ref. [28]). To study whether astigmatism can also lead to multiple filamentation, we consider the input beam

$$A_+^0(x,y)=2\sqrt{CN_c^{\mathrm{circ}}}\exp[-(ex)^2-y^2], \quad (39)$$

where C is constant and e is input astigmatism parameter ($e=1$ corresponds to a cylindrically symmetric input beam). Our simulations of Eq. (36) show that input astigmatism can lead to multiple filamentation when the input power is several times N_c^{circ}.[14] For example, Fig. 13 shows astigmatic input beams that break up into two and three filaments. As with noise-initiated multiple filamentation, during further propagation, each of the filaments undergoes focusing-defocusing oscillations and is roughly cylindrically symmetric.

IX. COMPARISON OF CIRCULAR AND LINEAR POLARIZATION

It is instructive to compare the results of circularly polarized input beams with those of linearly polarized ones. In Ref. [8], we showed that when the input beam is linearly polarized in the x direction and $f\ll 1$, Eqs. (1) and (2) can be approximated with the scalar equation

[13] A closer inspection of the results reveals that after the breakup has occurred, each of the filaments undergoes focusing-defocusing oscillations, as predicted by modulation theory (see Sec. VI) and is roughly cylindrically symmetric (see Fig. 12).

[14] We note that the effective threshold power for collapse of astigmatic beams is higher than for cylindrically symmetric beams by a factor of $\approx[0.2(e+1/e)+0.6]$, see Ref. [12].

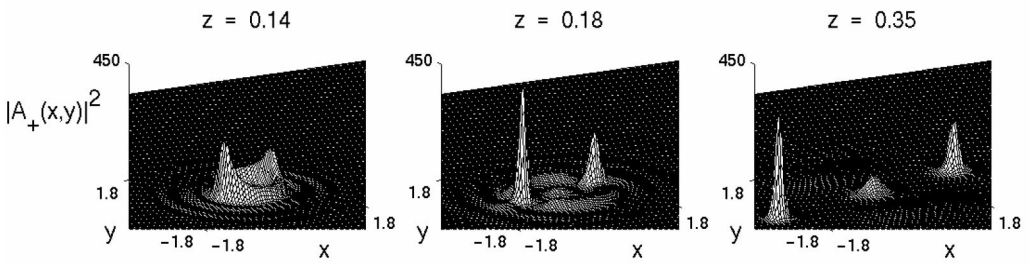

FIG. 10. Intensity of the solution of Eq. (36) with $f=0.05$ and the noisy input beam (38) with $c=0.1$ and $N(0)=10N_c^{\mathrm{circ}}$.

$$iA_{1,z}+\Delta_\perp A_1+|A_1|^2A_1=-f^2\left[\underbrace{\frac{1}{4}A_{1,zz}}_{\text{nonparax.}}+\underbrace{\frac{4+6\gamma}{1+\gamma}|A_{1,x}|^2A_1+(A_{1,x})^2A_1^*+\frac{1+2\gamma}{1+\gamma}(|A_1|^2A_{1,xx}+A_1^2A_{1,xx}^*)}_{\text{vectorial effects}}\right], \tag{40}$$

where the variables are rescaled according to Eq. (15) and A_1 is the nondimensional amplitude in the x direction. When $f=0$, Eq. (40) reduces to the NLS equation (4). The $A_{1,zz}$ term is the nonparaxial term (in the scalar nonlinear Helmholtz equation for A_1) and the remaining terms on the right-hand side correspond to the combined effects of the linear and nonlinear couplings of $\mathcal{E}_1$ to $\mathcal{E}_3$ and the contribution of E_1 in the grad-div term in Eqs. (1) and (2).[15]

Setting $f=0$ in Eq. (40) and $f=\varepsilon=0$ in Eq. (19) shows that for positive values of γ, the threshold power for self-focusing of circularly polarized beams is higher by $(1+\gamma)$ than for linearly polarized ones, see Eq. (30). In addition, we recall that γ does not appear in Eq. (24a). Therefore, when $\mathcal{E}_-^0$ is negligible then, to leading order, the constant γ does not affect the beam dynamics, other than to increase the threshold power. In contrast, γ cannot be ''factored out'' of Eq. (40) for *linearly* polarized input beams.

A. Asymptotic analysis

Applying modulation theory to Eq. (40) for linearly polarized beams leads to the same reduced system (32) as for circularly polarized beams, the only difference being that $C_{\mathrm{vec}}\approx 16/3$ for circular-polarization, whereas $C_{\mathrm{vec}}(\gamma)\approx(16/3)[1+\gamma/(1+\gamma)]$ for linearly polarized beams [8]. Thus, for both circularly polarized and linearly polarized beams, vectorial effects are considerably stronger than nonparaxiality, and both arrest collapse and lead to focusing-defocusing oscillations. In both cases, the effect of coupling to the second transverse field (i.e., E_2 or E_-) is negligible.

In the case of linear polarization, the $O(f^2)$ terms in the reduced PDE (40) correspond, in part, to the contribution of $\mathcal{E}_1$ to the grad-div term, which does not vanish even when $\mathcal{E}_2\equiv\mathcal{E}_3\equiv 0$. Similarly, in the case of circular-polarization the $O(f^2)$ terms in Eq. (19a) correspond, in part, to the contribution of $\mathcal{E}_+$ to the grad-div term, which does not vanish even when $\mathcal{E}_-\equiv\mathcal{E}_3\equiv 0$. A closer inspection of the derivation of the corresponding reduced systems reveals that the constants corresponding to the contribution $\mathcal{E}_1$ and $\mathcal{E}_+$ to the grad-div term are $C_{\vec\nabla(\vec\nabla\cdot(E_1,0,0))}=C_{\vec\nabla(\vec\nabla\cdot(E_+,0,0))}\approx 8$. Therefore, for both linear and circular-polarizations, the contribution of $\mathcal{E}_1$ or $\mathcal{E}_+$ in the grad-div term is a defocusing mechanism that is *eight times stronger* than nonparaxiality. Perhaps surprisingly, the coupling to $\mathcal{E}_3$ is considerably weaker than the contribution of $\mathcal{E}_1$ or $\mathcal{E}_+$ in the grad-div term, and this coupling is *focusing*: for linear polarization it is focusing for $\gamma<1$, because $C_{E_3}(\gamma)\approx-(8/3)(1-\gamma)/(1+\gamma)$ [25], and for circular-polarization it is focusing independent of γ, because $C_{E_3}\approx-8/3$. As we remarked at the end of Sec. VI, these results are surprising to the extent that the interpretation of the results of previous studies suggested that the coupling to $\mathcal{E}_3$ is a defocusing mechanism. In contrast, our study shows that the dominant vectorial effect is the contribution of $\mathcal{E}_1$ or $\mathcal{E}_+$ to the grad-div term, whereas the coupling to $\mathcal{E}_3$ is, in fact, weakly focusing. In retrospect, the observation that the coupling to $\mathcal{E}_3$ is weakly focusing is not so surprising, as the coupling to $\mathcal{E}_-$ in the case of circular-polarization is also weakly focusing.

B. Multiple filamentation

In Ref. [25], we pointed out that the preferred direction induced by linear polarization of an input beam breaks up the cylindrical symmetry in the vector Helmholtz model (1). Numerical simulations show that this symmetry breaking,

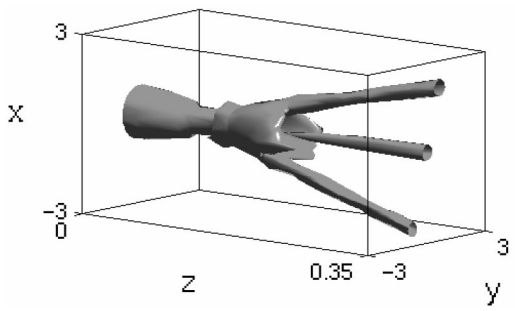

FIG. 11. Isosurface of $|A_+|^2$ of the solution in Fig. 10.

[15]The coupling to $\mathcal{E}_2$ is $O(f^4)$.

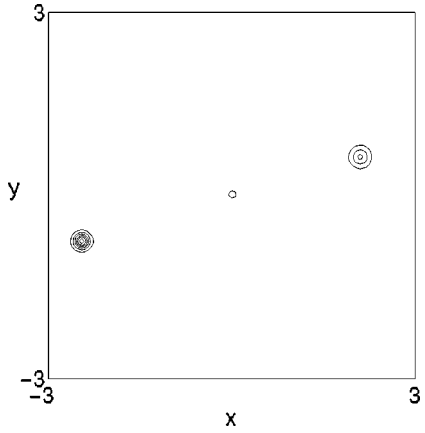

FIG. 12. Contour plot of $|A_+(x,y,z=0.35)|$ of the solution of Fig. 10.

which is manifested by the anisotropic $O(f^2)$ terms in Eq. (40), can lead to multiple filamentation, even when the input profile is perfectly cylindrically symmetric, i.e., $\mathcal{E}_1^0=\mathcal{E}_1^0(r)$ and $\mathcal{E}_2^0=0$. In contrast, circular-polarization does not induce a preferred direction. Therefore, a cylindrically symmetric circularly polarized beam would not undergo multiple filamentation (Corollary 3). Moreover, Corollary 4 suggests that even almost circularly polarized, cylindrically symmetric beams are unlikely to undergo multiple filamentation because the anisotropic terms are much weaker $[O(\varepsilon f^2)]$.

In Ref. [25], we tested numerically the original Bespalov-Talanov model for multiple filamentation, by solving the *unperturbed* NLS equation (4) with high-power cylindrically symmetric Gaussian input beams, to which we added random noise (38). We saw neither evidence for multiple filamentation nor even for mild instabilities. Rather, the beams converged to a cylindrically symmetric profile and collapsed. However, when additional physical mechanisms, such as saturation of the Kerr nonlinearity, are added to the NLS model, then input noise can lead to multiple filamentation of very high-power input beams (see Ref. [25], and references therein). For circularly polarized beams, we reach similar conclusions: When we solve the Close *et al.* model (9) with high-power noisy input beams, the beams collapse while converging to a cylindrically symmetric profile (see Sec. VIII B). However, when nonparaxiality and the coupling to the axial component are included, input noise can lead to multiple filamentation of circularly polarized input beams. Thus, an essential requirement for noise to lead to multiple filamentation is the presence of an additional regularizing mechanism (such as nonlinear saturation, nonparaxiality, vectorial effects, or plasma formation) that arrests the collapse and lead to an (unstable) ring structure.

X. FINAL REMARK

For over 35 years, studies of self-focusing of circularly polarized beams followed Close *et al.* [2] and used system (9). These studies have led to controversial results regarding circular-polarization stability. In this study, we show that the assumptions on which the Close *et al.* model is based are not valid physically. While some insight can be gained from system Eq. (9), this system can lead to wrong predictions. In this study, we derive a mathematical model for circularly polarized input beams, which takes into account nonparaxiality and vectorial effects. Based on this model, we conclude that circular polarization is stable.

Our study also shows that cylindrically symmetric circularly polarized input beams will not undergo multiple filamentation; that a small deviation from a circular-polarization state is unlikely to lead to multiple filamentation, but that input-beam noise or astigmatism can lead to multiple filamentation of circularly polarized beams. Therefore, suppression of multiple filamentation of *circularly polarized* beams should focus on producing a cylindrically symmetric input profile, rather than on producing a perfect circular-polarization state. In contrast, one cannot suppress multiple filamentation of *linearly polarized* beams by producing a cylindrically symmetric input profile because multiple filamentation can result from the preferred polarization direction induced by linear polarization.

ACKNOWLEDGMENT

This research was supported by Grant No. 2000311 from the United States–Israel Binational Science Foundation (BSF), Jerusalem, Israel.

APPENDIX: DERIVATION OF EQ. (19)

The starting point for the derivation of Eq. (19) is Eqs. (16), which were also used in the derivation of Eq. (40) in Ref. [8]. Below we omit the technical details that were already obtained in Ref. [8] or that are similar to the derivation there (see Ref. [8], Appendixes).

1. Derivation of estimates (18)

We assume that the input beam is almost left-circularly polarized (13), i.e., that $A_-^0 \ll A_+^0$ and $A_3^0 \ll A_+^0$. Therefore, it follows from Eqs. (16) that over propagation distances of several diffraction lengths

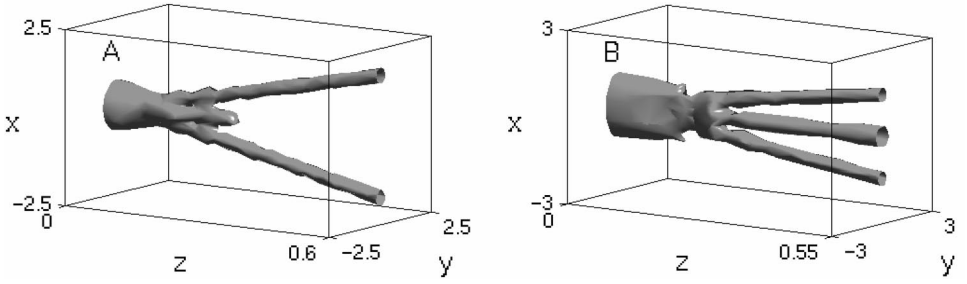

FIG. 13. Isosurface of $|A_+|^2$ of the solutions of Eq. (36) with $f=0.05$ and astigmatic input beams (39) with (a) $C=7.5$ and $e=0.9$ [i.e., $N(0)=8.3N_c^{\mathrm{circ}}$]; (b) $C=3.75$ and $e=0.6$ [i.e., $N(0)=6.25N_c^{\mathrm{circ}}$].

$$A_+(x,y,z)=O(1),\quad A_-(x,y,z)=o(1),\quad A_3(x,y,z)=o(1). \tag{A1}$$

In analogy with system Eq. (9), we define the nondimensional circular nonlinear polarizations

$$N_\pm=\frac{1}{\sqrt{2}}(N_1\pm iN_2), \tag{A2}$$

where $\vec{N}=(N_1,N_2,N_3)$ is defined in Eq. (16c).

Similar to the derivation in Ref. [8], it follows from Eqs. (16b), (16c), and (A1) that

$$A_3=O(f). \tag{A3}$$

Using Eq. (A3), we get from Eq. (16c) that

$$N_3=O(f). \tag{A4}$$

Therefore, substituting Eq. (A4) in Eq. (16a) gives that

$$iA_{1,z}+\Delta_\perp A_1+\tfrac{1}{4}f^2A_{1,zz}+N_1=-f\partial_x(f\vec{\nabla}_\perp\cdot\vec{N}+iN_3)+O(f^4) \tag{A5a}$$

and

$$iA_{2,z}+\Delta_\perp A_2+\tfrac{1}{4}f^2A_{2,zz}+N_2=-f\partial_y(f\vec{\nabla}_\perp\cdot\vec{N}+iN_3)+O(f^4). \tag{A5b}$$

Subtracting Eq. (A5b) from i times Eq. (A5a), dividing by $\sqrt{2}$, and using Eq. (A2) gives that

$$iA_{-,z}+\Delta_\perp A_-+\tfrac{1}{4}f^2A_{-,zz}+N_-=O(f^2). \tag{A6}$$

Throughout the derivation in this appendix, we use the following identities, whose proof is straightforward:

$$\begin{aligned}\vec{A}\cdot\vec{A}^*&=|A_1|^2+|A_2|^2+|A_3|^2\\&=|A_+|^2+|A_-|^2+|A_3|^2\quad[\text{from Eq. (17)}],\\ \vec{A}\cdot\vec{A}&=A_1^2+A_2^2+A_3^2=2A_+A_-+A_3^2\quad[\text{from Eq. (17)}],\end{aligned} \tag{A7}$$

and

$$A_1=\frac{1}{\sqrt{2}}(A_++A_-),$$

$$A_2=-\frac{i}{\sqrt{2}}(A_+-A_-)\quad[\text{from Eq. (17)}]. \tag{A8}$$

It follows from Eqs. (17), (16c), (A2), and (A7) that

$$\begin{aligned}N_-&=\frac{1}{1+\gamma}[(\vec{A}\cdot\vec{A}^*)A_-+\gamma(\vec{A}\cdot\vec{A})A_+^*]\\&=\frac{1}{1+\gamma}[(|A_+|^2+|A_-|^2+|A_3|^2)A_-\\&\quad+\gamma(2A_+A_-+A_3^2)A_+^*]\quad[\text{from Eq. (17)}].\end{aligned} \tag{A9}$$

Therefore, we get from Eqs. (A3) and (A9) that

$$N_-=\frac{1}{1+\gamma}[(1+2\gamma)|A_+|^2+|A_-|^2]A_-+O(f^2). \tag{A10}$$

We can rewrite Eq. (A6) using estimate (A10) as

$$\left(i\partial_z+\Delta_\perp+\frac{1+2\gamma}{1+\gamma}|A_+|^2+\frac{1}{1+\gamma}|A_-|^2\right)A_-=O(f^2). \tag{A11}$$

We note that Eq. (A11) is a homogeneous equation in A_- with an $O(1)$ operator on the left- hand side. Since $A_-^0/A_+^0=O(\varepsilon)$ [Eqs. (A1)] and the driving terms on the right-hand side of Eq. (A11) are $O(f^2)$, estimate (18a) follows.

Using Eq. (16b), we get from Eqs. (A3) and (A4) that

$$A_3=if(A_{1,x}+A_{2,y})+O(f^3). \tag{A12}$$

Using Eq. (18a), we obtain from identities (A8) that

$$A_1=\frac{1}{\sqrt{2}}A_++O(f^2,\varepsilon),\quad A_2=-\frac{i}{\sqrt{2}}A_++O(f^2,\varepsilon). \tag{A13}$$

Substituting Eq. (A13) into Eq. (A12) yields estimate (18b).

2. Derivation of Eq. (19)

In order to obtain Eq. (19b), we first use Eq. (18a) to get that

$$|A_-|^2A_-=O(f^6,\varepsilon^3). \tag{A14}$$

Equation (19b) follows from substituting estimate (A14) into Eq. (A11).

Below we derive Eq. (19a). Summing Eq. (A5b) with i times Eq. (A5a) and dividing by $\sqrt{2}$ leads to

$$\begin{aligned}&iA_{+,z}+\Delta_\perp A_++\frac{1}{4}f^2A_{+,zz}+N_+\\&\quad=-\frac{f}{\sqrt{2}}(\partial_x+i\partial_y)(f\vec{\nabla}_\perp\cdot\vec{N}+iN_3)+O(f^4).\end{aligned} \tag{A15}$$

Using identities (A7) and estimates (18), it follows that

$$\begin{aligned}N_+&=\frac{1}{1+\gamma}[(\vec{A}\cdot\vec{A}^*)A_++\gamma(\vec{A}\cdot\vec{A})A_-^*]\quad[\text{from Eq. (16c)}],\\&=\frac{1}{1+\gamma}[(|A_+|^2+|A_-|^2+|A_3|^2)A_++\gamma(2A_+A_-\\&\quad+A_3^2)A_-^*]\quad[\text{from Eq. (A7)}],\end{aligned}$$

$$= \frac{1}{1+\gamma}|A_+|^2A_+ + \frac{1+2\gamma}{1+\gamma}|A_-|^2A_+ + \frac{f^2}{2(1+\gamma)}|(i\partial_x + \partial_y)A_+|^2A_+ + O(f^4,\varepsilon f^2) \quad \text{[from Eq. (18)]}, \tag{A16}$$

and that

$$\vec{A}\cdot\vec{A}^* = |A_+|^2 + |A_-|^2 + |A_3|^2 = |A_+|^2 + O(f^2,\varepsilon^2) \quad \text{[from Eqs. (A7) and (18)]},$$

$$\vec{A}\cdot\vec{A} = 2A_+A_- + A_3^2 = O(f^2,\varepsilon) \quad \text{[from Eqs. (A7) and (18)]}. \tag{A17}$$

Similarly, we obtain that

$$N_3 = \frac{1}{1+\gamma}[(\vec{A}\cdot\vec{A}^*)A_3 + \gamma(\vec{A}\cdot\vec{A})A_3^*] \quad \text{[from Eq. (16c)]},$$

$$= \frac{1}{1+\gamma}|A_+|^2A_3 + O(f^3,\varepsilon f)$$

$$= \frac{if}{\sqrt{2}(1+\gamma)}|A_+|^2(\partial_x - i\partial_y)A_+ + O(f^3,\varepsilon f) \quad \text{[from Eqs. (A17) and (18b)]}, \tag{A18}$$

and that

$$\vec{\nabla}_\perp\cdot\vec{N} \equiv N_{1,x} + N_{2,y} = \frac{1}{1+\gamma}\partial_x[(\vec{A}\cdot\vec{A}^*)A_1 + \gamma(\vec{A}\cdot\vec{A})A_1^*] + \frac{1}{1+\gamma}\partial_y[(\vec{A}\cdot\vec{A}^*)A_2 + \gamma(\vec{A}\cdot\vec{A})A_2^*] \quad \text{[from Eq. (16c)]},$$

$$= \frac{1}{1+\gamma}\partial_x(|A_+|^2A_1) + \frac{1}{1+\gamma}\partial_y(|A_+|^2A_2) + O(f^2,\varepsilon) \quad \text{[from Eq. (A17)]},$$

$$= \frac{1}{\sqrt{2}(1+\gamma)}\partial_x(|A_+|^2A_+) - \frac{i}{\sqrt{2}(1+\gamma)}\partial_y(|A_+|^2A_+) + O(f^2,\varepsilon) \quad \text{[from Eq. (A13)]},$$

$$= \frac{1}{\sqrt{2}(1+\gamma)}(\partial_x - i\partial_y)(|A_+|^2A_+) + O(f^2,\varepsilon). \tag{A19}$$

Substituting Eqs. (A16), (A18), and (A19) into Eq. (A15) leads to

$$iA_{+,z} + \Delta_\perp A_+ + \frac{1}{1+\gamma}|A_+|^2A_+ + \frac{1+2\gamma}{1+\gamma}|A_-|^2A_+ = -\frac{1}{4}f^2A_{+,zz} - \frac{f^2}{2(1+\gamma)}|(i\partial_x + \partial_y)A_+|^2A_+ - \frac{f^2}{2(1+\gamma)}(\partial_x + i\partial_y)[(\partial_x - i\partial_y)(|A_+|^2A_+) - |A_+|^2(\partial_x - i\partial_y)A_+] + (f^4,\varepsilon f^2).$$

Rearranging the right-hand side of this equation gives Eq. (19a).

[1] P.L. Kelley, Phys. Rev. Lett. **15**, 1005 (1965).
[2] Y.R. Shen, Prog. Quantum Electron. **4**, 1 (1975).
[3] D.H. Close, C.R. Giuliano, R.W. Hellwarth, L.D. Hess, F.J. McClung, and W.G. Wagner, IEEE J. Quantum Electron. **QE-2**, 553 (1966).
[4] A. Braun, G. Korn, X. Liu, D. Du, J. Squier, and G. Mourou, Opt. Lett. **20**, 73 (1995).
[5] A. Brodeur, F.A. Ilkov, and S.L. Chin, Opt. Commun. **129**, 193 (1996).
[6] N.F. Pilipetskii and A.R. Rustamov, Pis'ma Zh. Éksp. Teor. Fiz. **2**, 88 (1965) [JETP Lett. **2**, 55 (1965)].
[7] V.I. Bespalov and V.I. Talanov, Pis'ma Zh. Éksp. Teor. Fiz. **3**, 471 (1966) [JETP Lett. **3**, 307 (1966)].
[8] G. Fibich and B. Ilan, Physica D, **157**, 113 (2001).
[9] R. W. Boyd, *Nonlinear Optics* (Academic Press, Boston, 1992).
[10] P.D. Maker, R.W. Terhune, and C.M. Savage, Phys. Rev. Lett. **12**, 507 (1964).
[11] G. Fibich and A. Gaeta, Opt. Lett. **25**, 335 (2000).
[12] G. Fibich and B. Ilan, J. Opt. Soc. Am. B, **17**, 1749 (2000).
[13] M.I. Weinstein, Commun. Math. Phys. **87**, 567 (1983).
[14] G. Fibich and G.C. Papanicolaou, SIAM (Soc. Ind. Appl. Math.) J. Appl. Math., **60**, 183 (1999).
[15] C. Sulem and P.L. Sulem, *The Nonlinear Schrödinger Equation* (Springer, New York, 1999).
[16] Y. R. Shen, *The Principles of Nonlinear Optics* (Wiley, New York, 1984).
[17] W.G. Wagner, H.H. Haus, and J.H. Marburger, Phys. Rev. **175**,

256 (1968).
[18] H. Prakash and N. Chandra, Nuovo Cimento B **57**, 255 (1968).
[19] D.V. Vlasov, V.V. Korobkin, and R.V. Serov, Kvant. Elektron. (Moscow) **6**, 1542 (1979) [Quantum Electron. **9**, 904 (1979)].
[20] Y.H. Meyer, Opt. Commun. **34**, 439 (1980).
[21] C.H. Skinner and P.D. Kleiber, Phys. Rev. A **21**, 151 (1980).
[22] I. Golub, R. Shuker, and G. Erez, Opt. Commun. **57**, 143 (1986).
[23] A.L. Berkhoer and V.E. Zakharov, Zh. Éksp. Teor. Fiz. **58**, 903 (1970) [Sov. Phys. JETP **31**, 486 (1970)].
[24] G. Fibich and G.C. Papanicolaou, Phys. Lett. A, **239**, 167 (1998).
[25] B. Ilan, Ph.D. thesis, School of Mathematical Sciences, Tel Aviv University, 2003.
[26] G. Fibich, Phys. Rev. Lett. **76**, 4356 (1996).
[27] S. Chi and Q. Guo, Opt. Lett. **20**, 1598 (1995).
[28] J.L. Blows, J.M. Dawes, and P.A. Piper, Opt. Commun. **162**, 247 (1999).